

University of Wollongong

Research Online

---

Faculty of Engineering and Information  
Sciences - Papers: Part B

Faculty of Engineering and Information  
Sciences

---

2018

## In-field and out-of-file application in $^{12}\text{C}$ ion therapy using fully 3D silicon microdosimeters

Linh T. Tran

*University of Wollongong*, tltran@uow.edu.au

Lachlan Chartier

*University of Wollongong*, lc752@uowmail.edu.au

David Bolst

*University of Wollongong*, dbolst@uow.edu.au

Jeremy A. Davis

*University of Wollongong*, jeremyd@uow.edu.au

Dale A. Prokopovich

*University of Wollongong*, dalep@uow.edu.au

*See next page for additional authors*

Follow this and additional works at: <https://ro.uow.edu.au/eispapers1>



Part of the [Engineering Commons](#), and the [Science and Technology Studies Commons](#)

---

### Recommended Citation

Tran, Linh T.; Chartier, Lachlan; Bolst, David; Davis, Jeremy A.; Prokopovich, Dale A.; Pogosso, Alex; Guatelli, Susanna; Reinhard, Mark I.; Petasecca, Marco; Lerch, Michael L. F; Matsufuji, Naruhiro; Povoli, Marco; Summanwar, Anand; Kok, Angela; Jackson, Michael A.; and Rosenfeld, Anatoly B., "In-field and out-of-file application in  $^{12}\text{C}$  ion therapy using fully 3D silicon microdosimeters" (2018). *Faculty of Engineering and Information Sciences - Papers: Part B*. 1851.  
<https://ro.uow.edu.au/eispapers1/1851>

Research Online is the open access institutional repository for the University of Wollongong. For further information contact the UOW Library: [research-pubs@uow.edu.au](mailto:research-pubs@uow.edu.au)

---

## In-field and out-of-file application in $^{12}\text{C}$ ion therapy using fully 3D silicon microdosimeters

### Abstract

This paper presents recent development of Silicon on Insulator (SOI) detectors for microdosimetry at the Centre for Medical Radiation Physics (CMRP) at the University of Wollongong. A new CMRP SOI microdosimeter design, the 3D mushroom microdosimeter is presented. Modification of SOI design and changes to the fabrication processes have led to improved definition of the microscopic sensitive volumes (SV), and thus to better modelling of the deposition of ionizing energy in a biological cell. The electrical and charge collection properties of the devices have been presented in previous works. In this study, the response of the microdosimeters in monoenergetic and spread out Bragg peak therapeutic  $^{12}\text{C}$  ion beam at Heavy Ion Medical Accelerator in Chiba (HIMAC, Japan) are presented. Derived relative biological effectiveness (RBE) in  $^{12}\text{C}$  ion radiation therapy matches the tissue equivalent proportional counter (TEPC) well, along with outstanding spatial resolution. The use of SOI technology in experimental microdosimetry offers simplicity (no gas system or HV supply), high spatial resolution, low cost, high count rates capabilities for beam characterisation and quality assurance (QA) in charged particle therapy.

### Disciplines

Engineering | Science and Technology Studies

### Publication Details

Tran, L. T., Chartier, L., Bolst, D., Davis, J., Prokopovich, D. A., Pogosso, A., Guatelli, S., Reinhard, M. I., Petasecca, M., Lerch, M. L. F., Matsufuji, N., Povoli, M., Summanwar, A., Kok, A., Jackson, M. & Rosenfeld, A. B. (2018). In-field and out-of-file application in  $^{12}\text{C}$  ion therapy using fully 3D silicon microdosimeters. *Radiation Measurements*, 115 55-59.

### Authors

Linh T. Tran, Lachlan Chartier, David Bolst, Jeremy A. Davis, Dale A. Prokopovich, Alex Pogosso, Susanna Guatelli, Mark I. Reinhard, Marco Petasecca, Michael L. F. Lerch, Naruhiro Matsufuji, Marco Povoli, Anand Summanwar, Angela Kok, Michael A. Jackson, and Anatoly B. Rosenfeld

# In-field and out-of-field application in $^{12}\text{C}$ ion therapy using fully 3D silicon microdosimeters

Linh T. Tran<sup>a</sup>, Lachlan Chartier<sup>a,b</sup>, David Bolst<sup>a</sup>, Jeremy Davis<sup>a,f</sup>, Dale A. Prokopovich<sup>a,b</sup>, Alex Pogosso<sup>a</sup>, Susanna Guatelli<sup>a,f</sup>, Mark I. Reinhard<sup>a,b</sup>, Marco Petasecca<sup>a,f</sup>, Michael L. F. Lerch<sup>a,f</sup>, Naruhiro Matsufuji<sup>c</sup>, Marco Povoli<sup>d</sup>, Anand Summanwar<sup>d</sup>, Angela Kok<sup>d</sup>, Michael Jackson<sup>e</sup> and Anatoly B. Rosenfeld<sup>a,f</sup>

<sup>a</sup>Centre for Medical Radiation Physics, University of Wollongong, NSW, 2522, Australia

<sup>b</sup>Ionising Radiation, NSTLI Nuclear Stewardship, Australian Nuclear Science and Technology Organization, Lucas Heights, NSW 2234, Australia

<sup>c</sup>National Institutes for Quantum and Radiological Science and Technology, Chiba, Japan

<sup>d</sup>SINTEF, Norway

<sup>e</sup>University of New South Wales, Sydney NSW 2052, Australia

<sup>f</sup>Illawarra Health Medical Research Institute, Australia

---

## HIGHLIGHTS

- ▶ The application of the silicon microdosimeters for radiation field characterisation in heavy ion therapy was presented
- ▶ Microdosimetric measurements and dose equivalent determination of penumbra for RBE<sub>10</sub> in  $^{12}\text{C}$  ion therapy

---

## ARTICLE INFO

### Article history:

Received Click here to enter the received date

Received in revised form Revised date

Accepted Accepted date

Available on line On-line date

---

### Keywords:

Microdosimetry

Relative biological efficiency (RBE)

Charged particle therapy

Silicon microdosimeter

3D sensitive volume

---

## ABSTRACT

This paper presents recent development of Silicon on Insulator (SOI) detectors for microdosimetry at the Centre for Medical Radiation Physics (CMRP) at the University of Wollongong. A new CMRP SOI microdosimeter design, the 3D mushroom microdosimeter is presented. Modification of SOI design and changes to the fabrication processes have led to improved definition of the microscopic sensitive volumes (SV), and thus to better modelling of the deposition of ionizing energy in a biological cell. The electrical and charge collection properties of the devices have been presented in previous works. In this study, the response of the microdosimeters in monoenergetic and spread out Bragg peak therapeutic  $^{12}\text{C}$  ion beam at Heavy Ion Medical Accelerator in Chiba (HIMAC, Japan) are presented. Derived relative biological effectiveness (RBE) in  $^{12}\text{C}$  ion radiation therapy matches the tissue equivalent proportional counter (TEPC) well, along with outstanding spatial resolution. The use of SOI technology in experimental microdosimetry offers simplicity (no gas system or HV supply), high spatial resolution, low cost, high count rates capabilities for beam characterization and quality assurance (QA) in charged particle therapy.

---

## 1 Introduction

Radiotherapy using heavy ion beams such as Carbon-ions is advantageous for the treatment of deep-seated tumors over conventional radiotherapy with X-rays due to an enhanced dose deposition in the Bragg peak (BP) at the end of the ion range. The high localization of dose delivery ensures the highest dose deposited in the tumour with minimal dose to the surrounding healthy tissue. Furthermore, the Relative Biological Effectiveness (RBE) of  $^{12}\text{C}$  ions used in hadron therapy greatly depends on the depth of the target volume in the body due to LET variation, nuclear fragmentation processes and neutron productions. Due to the complexity of the field, it is important to estimate the RBE of the heavy ions in hadron therapy applications so as to deliver the correct dose.

Microdosimetry is an extremely useful technique for estimating the RBE in unknown mixed radiation fields, typical for hadron therapy. The conventional detectors for microdosimetry is the tissue equivalent

proportional counter (TEPC) which shows advantages of isotropic response thanks to the spherical sensitive volume and tissue equivalence of walls and filling gas. However, the TEPC has several limitations such as high voltage operation, large size of assembly, which reduces spatial resolution and introduces wall effects, and an inability to simulate multiple cells.

The Centre for Medical Radiation Physics (CMRP) has developed multiple generations of microdosimeters on silicon-on-insulator (SOI) substrates which have been successfully tested [1-6] and recently summarized in [7]. The latest development of SOI microdosimeters at CMRP is the 3D array microdosimeter (also called "mushroom" microdosimeters) using 3D micro technology at SINTEF MiNaLab, Norway. The charge collection properties have been presented in [8].

This paper presents the response of the 3D mushroom microdosimeter in a therapeutic  $^{12}\text{C}$  ion beam in HIMAC, Japan and shows its application for relative biological effectiveness (RBE) determination in charged particle therapy.

## 1 2. Material and Method

### 2 Design of the 3D mushroom microdosimeter

Figure 1 shows a schematic of two different single 3D SV structures of the mushroom microdosimeters. The first structure is called a *trenched 3D* (or *air-trenched*) SV and consists of 3D cylindrical SVs with a core column of air and  $n^+$  doping in the inner walls of the SV center (Fig.1a). Each SV is surrounded with a trench of air and with  $p^+$  doping on the outer wall, designed to physically eliminate the possibility of charge generated outside the SV from being collected.

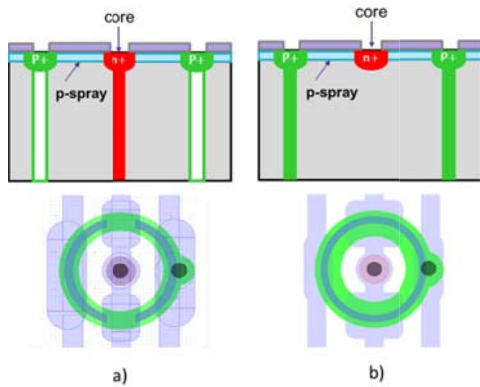


Figure 1 Schematics illustrating different configurations designed to define the sensitive volume geometry a) Trenched 3D structure (air-trenched) and b) Trenched planar structure (poly-trenched).

The second structure of the mushroom microdosimeter is called a *trenched planar* (or *poly-trenched*) SV, which also consists of 3D cylindrical SVs with a planar  $n^+$  core produced by ion implantation (planar technology). Each SV is surrounded with a completely  $p^+$  doped trench filled with polysilicon (Fig 1b).

The mushroom microdosimeter is based on an array of 2500 cylindrical SVs, each with a diameter of 30  $\mu\text{m}$  and a thickness of 9.1  $\mu\text{m}$ . The even and odd rows of SVs are read out independently to avoid events in adjacent sensitive volumes being read as a single event in the case of oblique charged particle tracks.

### Microdosimetric probe based on SOI microdosimeter

Figure 2 shows the microdosimetric probe, named the *Micro Plus* probe ( $\mu^+$ ), developed at the CMRP, based on an SOI microdosimeter with an array of 3D SVs connected to a low noise spectroscopy-based readout circuit. The readout electronics of the  $\mu^+$  probe are located 10 cm away from the detector to keep the readout circuitry out of the primary radiation field and avoid radiation damage to the electronics. The  $\mu^+$  probe is covered by a PMMA sheath to allow the microdosimeter to be operated in water.

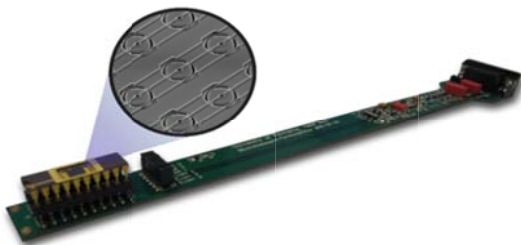


Figure 2 The microdosimetric probe (or also called MicroPlus probe)

Passive pristine Bragg Peak and Spread Out Bragg Peak (SOBP) of  $^{12}\text{C}$  ion beam delivery at HIMAC facility.

A 290MeV/u  $^{12}\text{C}$  ion beam was delivered with pristine BP used upstream to broaden the beam and was collimated to  $10 \times 10 \text{ cm}^2$  close to the phantom. The range of the 290MeV/u  $^{12}\text{C}$  beam in water after traveling through air between nozzle and phantom was 147.92mm. The microdosimetric probe was mounted in a water phantom using an X-Y stage to remotely control the detector location in the phantom with sub-hundred micron precision.

### Data collection and analysis

The spectral response of the detector was recorded with an Amptek MCA 8000A Multi Channel Analyzer (MCA). To obtain the microdosimetric quantities from the MCA spectrum, the energy deposited was converted to lineal energy which is used to describe the energy deposition in a micron sized sensitive volume (SV) along a particle's track, given by:

$$y = \frac{\varepsilon}{\langle l \rangle} \quad (1)$$

where  $\varepsilon$  is the energy deposited in a SV with an average chord length  $\langle l \rangle$ . A silicon-tissue scaling factor of 0.58 was obtained by calculating the energy deposition in silicon SV exposed to the 290MeV/u  $^{12}\text{C}$  ion radiation field, along the Bragg curve, by means of Geant4 [9].

Based on equation (1), the probability density  $f(y)$  can be measured for all primary and secondary particles generated during an exposure to tissue by ionizing radiation. The dose probability density  $d(y)$  is given by:

$$d(y) = \frac{y f(y)}{\bar{y}_F} \quad (2)$$

where  $\bar{y}_F = \int_0^\infty y f(y) dy$ ,  $\bar{y}_F$  is the frequency-mean lineal energy. The dose-mean lineal energy  $\bar{y}_D$  is defined as  $\bar{y}_D = \int_0^\infty y d(y) dy$ ; the latter is used to determine the  $\alpha$  parameter in the Linear Quadratic Model (LQM) applied for radiation field of interest and used later as an input parameter for the MKM to calculate RBE<sub>10</sub> corresponding to 10% of human salivary gland (HSG) cell survival. A detailed description for calculating RBE<sub>10</sub> using the MK model can be found in [10].

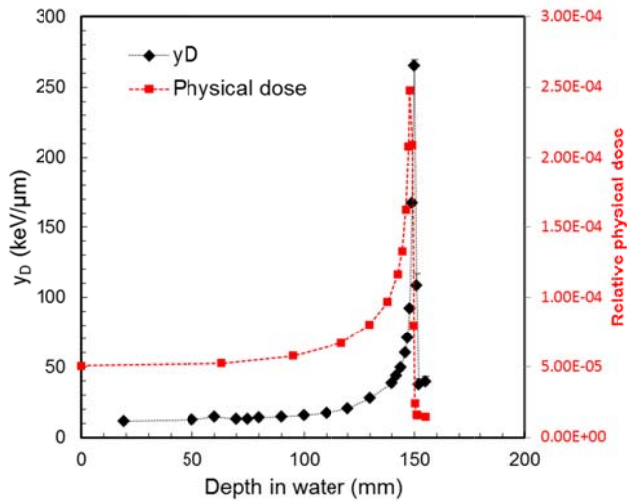
### Determination of Quality factor and dose equivalent in out-of-field measurements

The dose-equivalent H is defined as the product of the absorbed dose and a quality factor used to estimate the dose received by a person upon radiation exposure. Using the lineal energy dependent quality factor  $Q(y)$ , defined for radiation protection in the ICRU-40 report [11], the dose is scaled to be proportional to the biological effects it causes with respect to effects produced by a reference radiation. The method for calculating the dose-equivalent using microdosimetry has been explained in detail in previous work [12].

## 89 3. Results

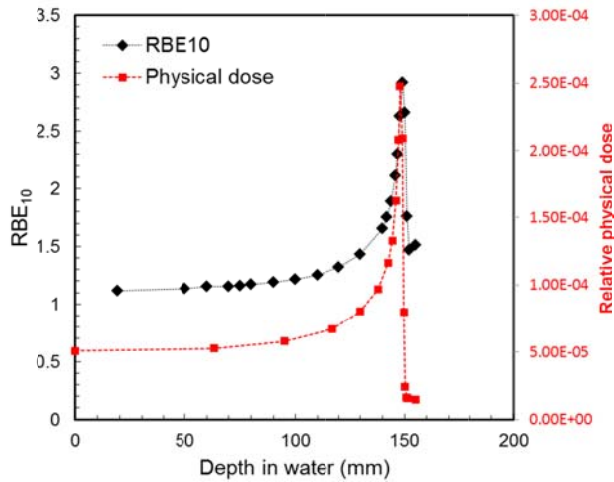
### 90 Response of the microdosimeter to 290MeV/u $^{12}\text{C}$ pristine BP

Figure 3 shows the dose-mean lineal energy values obtained at different depths in water obtained with the poly-trenched mushroom microdosimeter as well as the physical dose measured using a pin point ionisation chamber PTW31006 (0.015  $\text{cm}^3$  measuring volume) for the passively delivered 290MeV/u pristine  $^{12}\text{C}$  ion beam. The  $\bar{y}_D$  values at the entrance depth in water was 11.39keV/ $\mu\text{m}$  then increased up to approximately 90 keV/ $\mu\text{m}$  at the BP (147.92mm depth in water) and then sharply rose up to 265keV/ $\mu\text{m}$  at the distal part of the BP. This sharp increase in  $\bar{y}_D$  can only be obtained due to the extremely high spatial resolution of the SOI microdosimeter of an order of 10 $\mu\text{m}$  thick.



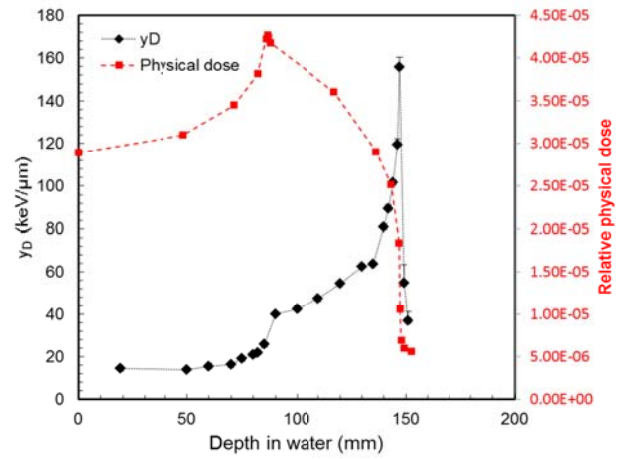
1  
2 Figure 3 Dose mean line energy obtained with poly-trenched  
3 mushroom microdosimeter and corresponding physical dose in  
4 response to 290MeV/u pristine <sup>12</sup>C ions.

5 Figure 4 shows the derived RBE<sub>10</sub> distribution obtained with the  
6 poly-trenched mushroom microdosimeter at different depths in water  
7 and corresponding physical dose, irradiated by a 290MeV/u pristine  
8 BP of <sup>12</sup>C ion beam. Fig. 4 shows that for pristine <sup>12</sup>C ions the  
9 maximum RBE<sub>10</sub> value of 2.92 occurs at the same depth as the  
10 physical dose, unlike other ions [13]. At the distal part of the BP when  
11 the maximum  $\bar{y}_D$  was approximately 265keV/μm, RBE<sub>10</sub> was about  
12 2.66. The decrease of RBE<sub>10</sub> towards the distal part of the BP is  
13 associated with the overkilling effect of cells which has been taken  
14 into account by the MK model [7].

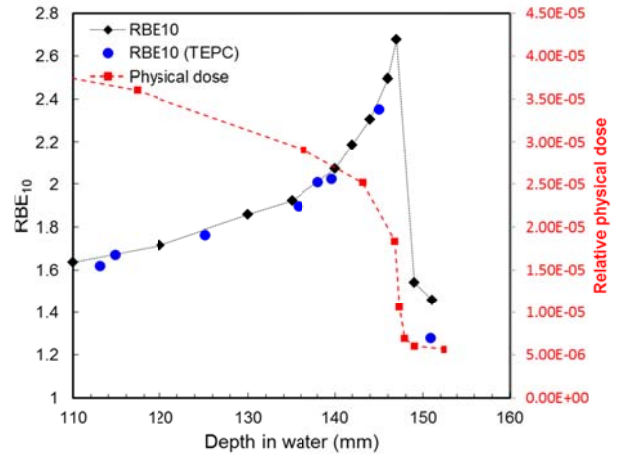


15

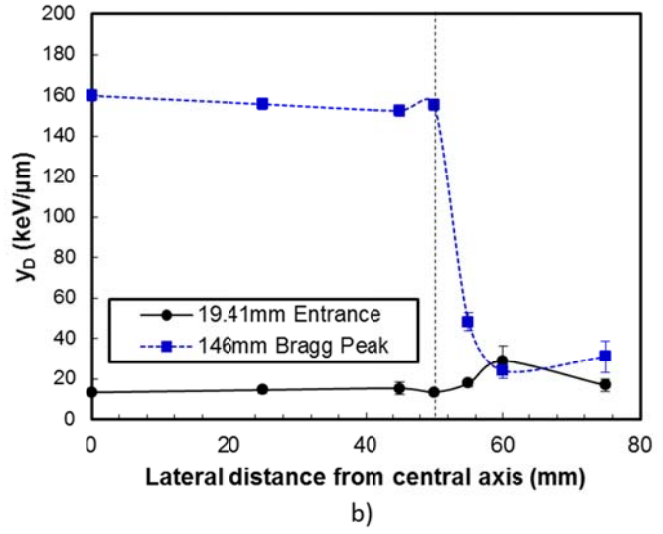
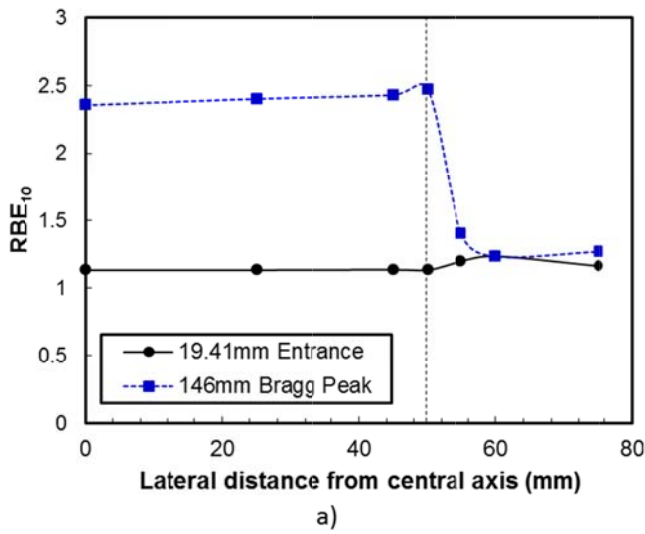
26 Figure 4 RBE<sub>10</sub> obtained from measurements with the poly-trenched  
27 mushroom microdosimeter in 290MeV/u pristine BP of <sup>12</sup>C ion beam.  
23  
24



25  
26 Figure 5 Dose mean line energy obtained with the poly-trenched  
27 mushroom microdosimeter and corresponding physical dose in  
28 response to 290MeV/u <sup>12</sup>C SOBP.  
29



30  
31 Figure 6 RBE<sub>10</sub> obtained from the measurements with the poly-  
32 trenched mushroom microdosimeter and TEPC and corresponding  
33 physical dose in 290MeV/u <sup>12</sup>C SOBP ions in water.  
34  
35  
36  
37



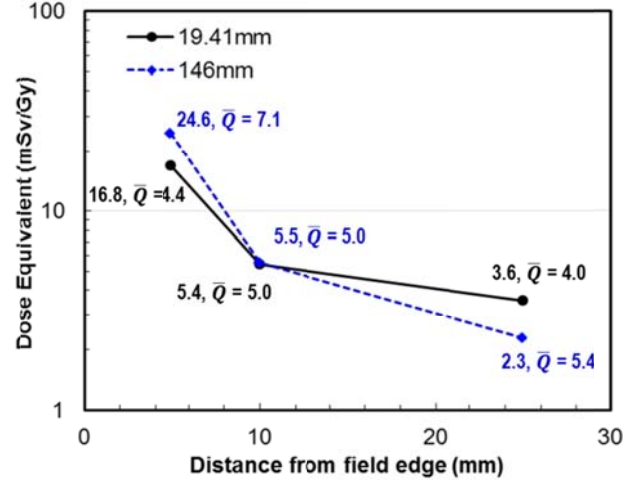
1  
2 Figure 7 RBE<sub>10</sub> (a) and  $\bar{y}_D$  (b) lateral distributions at 19.41mm and 146mm depth of 290MeV/u <sup>12</sup>C SOBPs in water where the field size was 10cm ×  
3 10cm. The vertical dashed line shown in the graphs indicates the edge of the radiation field.

4 Figure 5 and 6 show the  $\bar{y}_D$  and derived RBE<sub>10</sub> distributions in  
5 different depths in water obtained by the poly-trenched mushroom  
6 microdosimeter for a 290MeV/u 60mm <sup>12</sup>C SOBPs, respectively. The  
7 physical dose measured by the pinpoint ionisation chamber is also  
8 shown. In order to deliver a flat biological dose in the target region,  
9 the ridge filter delivers a physical dose which decreases with depth  
10 such that  $D_{biological} = D_{physical} \times RBE_{10}$  is flat over the 60mm treatment  
11 area. The maximum  $\bar{y}_D$  value obtained in the SOBPs <sup>12</sup>C ion beam of  
12 155.7keV/μm was observed to be lower than the maximum  $\bar{y}_D$  value in  
13 the <sup>12</sup>C pristine BP. This is due to the presence of the Al ridge filter  
14 which smears out the sharp dose at the BP region due to increased  
15 straggling.

16 Figure 7 shows the RBE<sub>10</sub> and  $\bar{y}_D$  lateral distributions at 19.41 mm  
17 and 146mm depth in water where the field size was 10cm × 10cm. The  
18 air-trenched mushroom microdosimeter was used for this measurement  
19 and it was placed at 0, 25, 45, 50, 55, 60 and 70mm from the central  
20 axis of the beam where 50mm lateral distance is the edge of the  
21 radiation field. At the entrance of the SOBPs (19.41mm depth), it can  
22 be seen that the RBE<sub>10</sub> values were almost constant in the field  
23 however at the penumbra region the RBE<sub>10</sub> slightly increased from  
24 1.13 to 1.23 as the microdosimeter moved 5 to 10mm out of the field  
25 due to fragments and neutrons. Finally the RBE<sub>10</sub> slightly decreased  
26 as the microdosimeter was moved further away.

27 At the end of the SOBPs region (146mm depth), the RBE<sub>10</sub> values  
28 were also almost constant in the field and then dropped sharply at the  
29 penumbra region. At 5mm distance from the edge of the field, the  
30 RBE<sub>10</sub> reduced from 2.47 down to 1.44 and stayed almost constant at  
31 further lateral distances due to the contribution of fragments with  
32 lower LET than that of the primary <sup>12</sup>C ions at the end of their range,  
33 but higher than recoiled protons, generated from neutrons. At larger  
34 distances, the effects of neutrons and fragmented protons are not  
35 distinguishable. A similar trend was observed with the  $\bar{y}_D$  distribution  
36 shown in Figure 7b. For 19.41mm depth both  $\bar{y}_D$  and RBE<sub>10</sub> are  
37 constant within the field while towards the edge of the field  $\bar{y}_D$  slightly  
38 decreases at 146mm depth leading to a slight increase in RBE<sub>10</sub> due to  
39 the correction for the overkilling effect by the MK model.  
40 The RBE<sub>10</sub> and  $\bar{y}_D$  values provide useful information on how the  
41 RBE<sub>10</sub> and  $\bar{y}_D$  varies at the penumbra region, particularly for the sharp  
42 dose gradients at the edge of the field.

53 Determination of dose equivalent in penumbra region of the  
54 290MeV/u <sup>12</sup>C beam



50  
61 Figure 8 Dose equivalent per Gy and calculated average quality factor  $\bar{Q}$   
62 at different lateral points from the edge of field for 19.41mm and  
63 146mm depth in water.

125 Figure 8 shows the dose equivalent per Gy in the middle of the  
126 SOBPs that was calculated based on measured lineal energy spectra  
127 obtained with the air-trenched mushroom microdosimeter at lateral  
128 distances of 5mm, 10mm and 25mm from the edge of the carbon  
129 SOBPs field for depths 19.41mm and 146mm. At 5 mm lateral from the  
130 field edge the dose equivalent was 24.6mSv/Gy and 16.8mSv/Gy for  
131 146mm and 19.41mm depth, respectively. The value of dose  
132 equivalent at these points correlate with average quality factor  $\bar{Q}$   
133 of 7.1 and 4.4 for 146mm and 19.41mm depth, respectively.  
134 Increasing  $\bar{Q}$  can be explained by the contribution of primary <sup>12</sup>C  
135 scattered ions which have lower energy at 146 mm depth in  
136 comparison to 19.41mm depth. At 10 mm lateral distance from the  
137 field edge the dose equivalent and  $\bar{Q}$  obtained at 2 depths were  
138 approximately the same. At 25 mm lateral distance the dose equivalent  
139 dropped faster laterally at 146mm depth in comparison with 19.41mm

1 depth while  $\bar{Q}$  is in opposite correlation with values of 5.4 and 4.0,  
 2 respectively. This can be explained due to larger partial contribution of  
 3 heavier fragments and fast neutrons at 146mm depth in comparison to  
 4 the shallower depth 19.41mm, while physical dose due to fragments is  
 5 lower at depth 146mm than at 19.41mm depth for this lateral point.

#### 6 4. Conclusion

7 Two SOI mushroom microdosimeters structures have been  
 8 recently developed, fabricated and characterised in pristine and SOBP  
 9  $^{12}\text{C}$  ion beams at HIMAC, Japan. The dose mean lineal energy and  
 10 RBE<sub>10</sub> distributions in water were obtained with exceptionally high  
 11 spatial resolution in the BP and the distal part of the BP. This work has  
 12 shown that the  $\bar{y}_D$  at the entrance of the  $^{12}\text{C}$  pristine BP (11.3keV/ $\mu\text{m}$ )  
 13 was lower than that obtained at the entrance of the SOBP  
 14 (14.5keV/ $\mu\text{m}$ ). However the maximum  $\bar{y}_D$  values in the pristine BP  
 15 was higher than those in the SOBP due to the presence of an Al ridge  
 16 filter. The maximum RBE<sub>10</sub> values for  $^{12}\text{C}$  ions occurred at the same  
 17 depth as the maximum physical dose in the BP which is in agreement  
 18 with other work [13]. This confirms the advantage of using  $^{12}\text{C}$  ion for  
 19 treatment of tumours.

20 The results obtained by the SOI microdosimeters show good  
 21 agreement with the TEPC after the application of proper correction  
 22 factors to convert the silicon response to that biological tissue and  
 23 indicate that the mushroom microdosimeter is suitable for use in heavy  
 24 ion therapy applications.

25 The lateral RBE<sub>10</sub> and dose mean lineal energy distributions were  
 26 obtained in this study for a depth close to the entrance and a depth at  
 27 the end of the SOBP. It has been shown that in the penumbra region  
 28 the lateral RBE<sub>10</sub> sharply decreased for 146mm depth and slightly  
 29 increased for 19.41mm depth. The dose equivalent at these lateral  
 30 points were also estimated. The dose equivalent reduced over a short  
 31 distance for lateral points at 19.41mm depth in comparison with  
 32 146mm depth.

33 The silicon microdosimeter containing 3D SVs presented in this  
 34 study is a new and fast radiation field characterisation tool that has  
 35 been tested and applied in heavy ion therapy applications with sub-  
 36 millimetre spatial resolution. It shows great promise as an  
 37 experimental device used for microdosimetric spectra measurements  
 38 and based on this, commissioning of RBE used in treatment planning  
 39 systems.

#### 41 Acknowledgement

42 This research was supported by the Australian Government  
 43 through the Australian Research Council's Discovery Projects funding  
 44 scheme (project DP 170102273).

45 The authors would like to acknowledge Dr. Nadia Court and her  
 46 team at the UNSW ANFF node for their packaging work as well as  
 47 Mr. Adam Sarbutt from NSTLI Nuclear Stewardship, ANSTO and Mr.  
 48 Peter Ihnat from the School of Physics, UOW for their assistance in  
 49 preparation for the experiment. Finally the authors would like to thank  
 50 all collaborators in the 3D-MiMiC project, funded by the Norwegian  
 51 Research Council via the NANO2021 program.

#### 52 References

53 [1] P. D. Bradley, "The development of a novel silicon  
 54 microdosimeter for High LET radiation therapy," Ph.D. dissertation,  
 55 Fac. Eng., Univ. Wollongong, Wollongong, Australia, 2000.  
 56 [2] A. L. Ziebell, W. H. Lim, M. I. Reinhard, I. Cornelius, D.  
 57 A. Prokopovich, R. Siegele, A. S. Dzurak, and A. B. Rosenfeld, "A  
 58 cylindrical silicon-on-insulator microdosimeter: charge collection  
 59 characteristics," IEEE Trans. Nucl. Sci., vol. 55, no. 6, pp. 3414-3420,  
 60 Dec. 2008.  
 61 [3] D. A. Prokopovich, M. I. Reinhard, G. C. Taylor, A. Hands,  
 62 A. B. Rosenfeld, "Comparison of SOI microdosimeter and tissue

63 equivalent proportional counter measurements at the CERF facility,"  
 64 IEEE Trans. Nucl. Sci., vol. 59, no. 5, pp. 2501-2505, 2012.

65 [4] J. Livingstone, D. A. Prokopovich, M. L. F. Lerch, M.  
 66 Petasecca, M. I. Reinhard, H. Yasuda, M. Zaider, J. Ziegler, V. L.  
 67 Pisacane, J. Dicello, V. Perevetaylo, and A. B. Rosenfeld, "Large area  
 68 silicon microdosimeter for dosimetry in high LET space radiation  
 69 fields: charge collection study," IEEE Trans. Nucl. Sci., vol. 59, no. 6,  
 70 pp. 3126-3132, Dec. 2012.

71 [5] L. T. Tran, Lachlan Chartier, Dale A. Prokopovich, Marco  
 72 Petasecca, Michael L. F. Lerch, Mark I. Reinhard, Vladimir  
 73 Perevetaylor, Nuruhiro Matsufuji and Anatoly B. Rosenfeld, "3D-mesa  
 74 "Bridge" silicon microdosimeter: charge collection study and  
 75 application to RBE studies in 12C radiation therapy," IEEE Trans.  
 76 Nucl. Sci., vol. 62, no. 2, pp. 504-511, Apr. 2015.

77 [6] L. T. Tran, Lachlan Chartier, David Bolst, Susanna Guatelli,  
 78 Mark I. Reinhard, Marco Petasecca, Michael L. F. Lerch, Vladimir L.  
 79 Pereverlaylo, Nuruhiro Matsufuji, David Hinde, Mahananda Dasgupta,  
 80 Andrew Stuchbery and Anatoly B. Rosenfeld, "3D Silicon  
 81 Microdosimetry and RBE study using  $^{12}\text{C}$  ion of different energies,"  
 82 IEEE Trans Nucl. Sci., vol. 62, no. 6, pp. 3027 – 3033, 2015.

83 [7] A. B. Rosenfeld, "Novel detectors for silicon based  
 84 microdosimetry, their concepts and applications," Nucl. Instrum.  
 85 Meth., Phys. Res. A, vol. 809, pp. 156–170, February 2016.

86 [8] Linh T. Tran, Lachlan Chartier, Dale A. Prokopovich, David  
 87 Bolst, Marco Povoli, Anand Summanwar, Angela Kok, Alex  
 88 Pogossov, Marco Petasecca, Susanna Guatelli, Mark I. Reinhard,  
 89 Michael Lerch, Mitchell Nancarrow, Nuruhiro Matsufuji, Michael  
 90 Jackson and Anatoly B. Rosenfeld, "Thin Silicon Microdosimeter  
 91 utilizing 3D MEMS Fabrication Technology: Charge Collection Study  
 92 and its application in mixed radiation fields," IEEE Trans Nucl. Sci.,  
 93 2017, DOI: 10.1109/TNS.2017.2768062.

94 [9] D. Bolst, S. Guatelli, L. T. Tran, L. Chartier, M. Lerch, N.  
 95 Matsufuji and A. Rosenfeld, "Correction factors to convert  
 96 microdosimetry measurements in silicon to tissue in  $^{12}\text{C}$  ion therapy,"  
 97 Phys. Med. Biol., vol. 62, no. 6, pp. 2055-2069, 2017.

98 [10] Kase Y, Kanai T, Matsumoto Y et al. "Microdosimetric  
 99 measurements and estimation of human cell survival for heavy-ion  
 100 beams". Radiation Res. 2006; 166:629–38.

101 [11] International Commission on Radiation Units and  
 102 Measurements, "The quality factor in radiation protection," Report  
 103 ICRU-40, 1986.

104 [12] Linh T. Tran Lachlan Chartier, David Bolst, Alex Pogossov,  
 105 Susanna Guatelli, Dale A. Prokopovich, Marco Petasecca, Michael L.  
 106 F. Lerch, Mark I. Reinhard, Benjamin Clasio, Nicolas Depauw, Hanne  
 107 Kooy, Jay Flanz, Aimee McNamara, Harald Paganetti, Chris Beltran,  
 108 Keith Furutani, Vladimir L. Perevertaylo, Michael Jackson and  
 109 Anatoly B. Rosenfeld. "Characterisation of proton pencil-beam  
 110 scanning using a high spatial resolution solid state microdosimeter",  
 111 Medical Physics, doi: 10.1002/mp.12563, 2017.

112 [13] G. Kraft "Tumor Therapy with Heavy Charged Particles",  
 113 Progress in Particle and Nuclear Physics 45(2000), 473-544

114